Assessment through first-principles calculations of an intermediate-band photovoltaic material based on Ti-implanted silicon: Interstitial versus substitutional origin

K. Sánchez, I. Aguilera, P. Palacios, and P. Wahnón
Departamento de Tecnologías Especiales, ETSI Telecomunicación and Instituto de Energía Solar, UPM, Ciudad Universitaria, Madrid 28040, Spain

(Received 23 December 2008; revised manuscript received 10 March 2009; published 10 April 2009)

Quantum calculations based on density-functional theory are carried out with the aim of discovering the origin of the electronic properties of Ti-implanted Si. This compound is a potential kind of intermediate-band photovoltaic material. Experimental results show a donor level at a few tenths of an eV below the conduction band for this compound. This could correspond to the electronic transition from an intermediate band to the conduction band of the host silicon. The structural, energetic, and electronic properties of several possible configurations appearing from the implantation of Ti on Si are calculated at different dilution levels in order to agree with the experimental conditions. Among the implantation processes, all of which are energetically unfavorable, interstitial Ti setting implies the energetic balance closest to the equilibrium, which agrees with the experimental measurements. Our conclusions predict that interstitial Ti atoms are responsible for the electronic transition found from the measurements, forecasting that a band fulfilling all the requirements of an intermediate-band material is formed in the compound. The optical absorption coefficient of an interstitially Ti-implanted Si compound is shown to illustrate the photoabsorption enhancement achieved in the main part of the solar spectrum with regard to bulk Si.

DOI: 10.1103/PhysRevB.79.165203 PACS number(s): 71.20.Nr, 71.15.Mb, 71.28.+d

I. INTRODUCTION

The emergence of the so-called third generation of solar cells is in progress. Among a number of novel proposals the intermediate-band (IB) solar cell concept[1] is one of the hot topics in current photovoltaic research. The intermediate-band photovoltaic material must have three electronic bands close to the Fermi level: valence band (VB) and conduction band (CB) as in a conventional semiconductor and also a narrow partially filled band placed into the host semiconductor gap and isolated from the aforementioned bands. Electrons can be promoted directly from the VB to the CB, as in usual semiconductors. Furthermore, photons with energies lower than the band gap can be absorbed by taking advantage of the IB in a two-step process. As a result, the photocurrent of the solar cell can be increased without decreasing the voltage.

Several crystalline materials have been proposed as intermediate-band materials in order to achieve a highly efficient device.[2–7] In most cases transition metals were introduced into host semiconductors, substituting group III atoms in such a way that 3*d* electrons of the transition metal can form the IB. Theoretical studies have concluded that the synthesis of several of these candidates is thus possible.[8] Even the first results of experimental samples have shown triple absorption spectra in accordance with quantum predictions.[9]

Meanwhile, other possible intermediate-band materials based on Si have been recently proposed in order to demonstrate experimentally the working principles of the intermediate-band solar cell. The clear advantage of Si as host semiconductor is the thorough knowledge of it, which could lead more proficiently to the first experimental devices.[10] For this reason Olea *et al.*[11] attempted to grow crystalline samples of Ti-implanted Si at concentrations significantly above the equilibrium solubility limit. They managed to synthesize a crystalline sample of Si with both interstitial and substitutional Ti with concentrations of 6×10^{19} and 10^{18} cm^{-3}, respectively. Both amounts are close or even above the so-called Mott limit, from which Ti atoms can form a band instead of isolated impurity levels. This prevents nonradiative Shockley-Reed-Hall recombinations.[12] Furthermore, a deep donor level with a concentration of 7×10^{17} cm^{-3} was obtained at 0.21 eV below the CB by means of an Arrhenius plot of the carrier concentration. In a later report,[13] the donor level was estimated to be at 0.36 eV below the CB by the same authors who carried out a simulation by means of a fitting of the sheet resistance.

The intention of this paper is twofold. On the one hand, it is intended to find the origin of the donor level by using first-principles quantum calculations. The structural, energetic, and electronic properties of the most probable products from a Ti-implanted Si compound, namely, interstitial and substitutional compositions, are analyzed in detail for this purpose. Furthermore, combinations of these situations are also considered.

On the other hand, the characteristics and position of the electronic states formed in all cases are examined to anticipate the possible formation of an intermediate-band photovoltaic material with the desired properties. In addition optical properties of a potential intermediate-band material close to the experimental conditions are computed. The improvement in the absorption coefficient across the solar spectrum produced by the IB is verified.

II. METHOD

Density-functional theory (DFT) calculations[14,15] were carried out to obtain atomic, electronic, and energetic properties of compounds based on Si doped with Ti at concentrations close to those of the experiment made by Olea *et al.*[13]

TABLE I. Structural parameters obtained from the relaxation carried out for substitutional Ti-derived compounds. Values are given in Å.

Compound	a	$d[Ti_{Si}\text{-}Si_{1st}]$	$d[Si_{\infty}\text{-}Si_{\infty}]$
$Ti_{Si}Si_{63}$	5.477	2.502	2.373
$Ti_{Si}Si_{215}$	5.468	2.504	2.368

TABLE II. Structural parameters obtained from the relaxation carried out for interstitial Ti-derived compounds. Values are given in Å.

Compound	a	$d[Ti_i\text{-}Si_{1st}]$	$d[Ti_i\text{-}Si_{2nd}]$	$d[Si_{\infty}\text{-}Si_{\infty}]$
Ti_iSi_{64}	5.471	2.481	2.772	2.368
Ti_iSi_{216}	5.466	2.474	2.774	2.366

Three different supercells of conventional Si_8 cubic unit cell were considered to include the Ti implantation: $2\times2\times2$ (Si_{64}), $3\times3\times3$ (Si_{216}), and $4\times4\times4$ (Si_{512}). The structures designed from the two former supercells were relaxed in order to observe the tendency of the corresponding impurities. Structural optimization for the compounds derived from Si_{512} was not carried out due to the amount of computational resources that would have been required for such number of atoms. Instead, the electronic structure was calculated for atomic coordinates extrapolated from those corresponding to the experimental bulk-Si lattice. As Sec. III will show, the electronic structures observed in the relaxation at low concentrations differ only slightly from the nonrelaxed results.

Generalized gradient approximation (GGA) with the PW91 parametrization[16] was used to treat the exchange-correlation potential in the plane-wave-based code VASP.[17,18] The energy cutoff established for the basis set was 245 eV. Projector augmented wave (PAW) potentials[19,20] were used to represent the inert core electrons. The samplings used to describe the Brillouin zone corresponding to the compounds derived from the $2\times2\times2$, $3\times3\times3$, and $4\times4\times4$ supercells were Γ-centered $6\times6\times6$, $4\times4\times4$, and $2\times2\times2$ grids, respectively. A Methfessel-Paxton first-order scheme[21] with 0.1 eV of smearing was chosen to extract the occupations of one-particle levels. The tetrahedron method[22] was used to obtain well-defined electronic densities of states (DOSs).

In the cases where ionic optimization was carried out, the atomic forces were minimized to below 0.01 eV/Å. Possible Jahn-Teller distortions produced by the implantation of Ti were treated during the relaxation study. This was done by carrying out additional calculations with slightly distorted coordinates and lattice parameters, hence preventing possible saddle point behavior of the starting guess caused by its high symmetry. The distorted relaxations evolved into the structures shown in Sec. III A, discarding therefore the Jahn-Teller distortions. The *dumbbell* split [110] structure, which is common among Si self-interstitial defects, evolved into a tetrahedral interstitial Ti configuration during the optimization. Additionally, no antiferromagnetic alignment of local magnetic moments was found energetically stable.

The optical behavior of the materials was characterized by means of their absorption coefficient derived from the dielectric function. The imaginary part of the latter was obtained by the sum on independent transitions between Kohn-Sham states, without local field effects, following the method described by Gajdoš *et al.*,[23] as implemented in the OPTICS code.[24] The real part of the dielectric function was obtained from the imaginary part by the Kramers-Kronig relations. To obtain the fully converged frequency-dependent dielectric properties of $3\times3\times3$ supercell based compounds, 250 empty bands were included, and the Brillouin zone was sampled using an $8\times8\times8$ Monkhorst-Pack grid including the Γ point.

III. RESULTS

A. Atomic structure of bulk-, Ti_{Si}-, and Ti_i-Si compounds

This work includes the optimized structures for bulk-Si- and Ti-implanted compounds, both in substitutional (Ti_{Si}) and interstitial (Ti_i) cases. The relaxed lattice parameter, a, of bulk Si turned out to be 5.464 Å for both Si_{64} and Si_{216} supercells, slightly longer than the experimental one (5.43 Å). This minor overestimation agrees with the tendency of GGA calculations. The resulting interatomic distances (2.366 Å) of both supercells agree down to thousandths of angstroms, as expected for correctly converged results.

The parameters of the relaxed Ti-substituted compounds are represented in Table I. The lattice parameter is expanded with regard to the bulk Si, marginally in the diluted $Ti_{Si}Si_{215}$ case and more noticeably for the most concentrated case, $Ti_{Si}Si_{63}$, as expected. In both compounds the substitution causes an increment of 0.14 Å in the distance to the first four nearest neighbors (Si_{1st}). The distances between the Si atoms placed in the remotest positions available in the cell (labeled as Si_{∞}) are 2.368 and 2.373 Å for $Ti_{Si}Si_{215}$ and $Ti_{Si}Si_{63}$, respectively. The latter is not close to the bulk relaxed interatomic distance. Therefore, the stress induced by the substitution is present along the whole cell. However, for the dilute case the Si_{∞}-Si_{∞} distance corresponds almost to the bulk one, being an indication that the implanted atom does not modify the bulk-Si structure at such a range.

The interstitial implantation of a Ti atom produces a more complex structure than the substitution, as can be seen in Table II. The four nearest neighbors at positions with a tetrahedral configuration appear at approximately 2.48 Å. However the six second nearest neighbors (Si_{2nd}) are placed rather close to the Ti atom, approximately 2.77 Å, in such a way that the crystalline field cannot be simplified only to the effect of the four nearest neighbors. This fact will be analyzed in Sec. III C 3.

The interatomic distances between the remotest Si atoms almost coincide with the bulk-Si ones, even for Ti_iSi_{64}. This indicates that the interstitial Ti modifies the bulk-Si structure throughout a smaller range than the substitutional Ti.

B. Formation energies

The formation energies of both kinds of Ti implantation were calculated from the total energies obtained for the com-

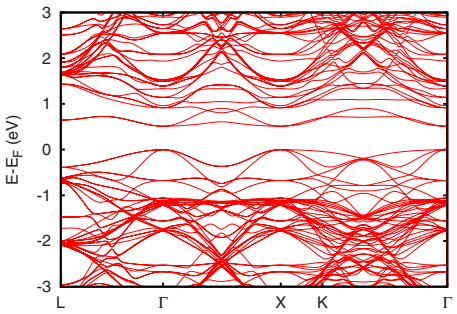

FIG. 1. (Color online) Band structure for the relaxed $Ti_{Si}Si_{63}$ compound.

pounds derived from the $3\times3\times3$ supercell, which is the largest cell allowed to be relaxed in the present study. The formation energy for the interstitial Ti_iSi_{216} compound was obtained using the equation

$$E^f[Ti_iSi_{216}] = E[Ti_iSi_{216}] - E[Si_{216}] - \frac{1}{2}E[Ti_2] = +1.51\ \text{eV},$$

where Ti_2 corresponds to the common hcp crystalline structure of Ti, made up of two atoms per formula. As a result, the formation of interstitial Ti involves a penalty of 1.51 eV/atom inserted.

In the case of the substitutional $Ti_{Si}Si_{215}$ compound, the formation energy balance corresponds to

$$E^f[Ti_{Si}Si_{215}] = E[Ti_{Si}Si_{215}] - \frac{215}{216}E[Si_{216}] - \frac{1}{2}E[Ti_2] = +2.16\ \text{eV}.$$

Therefore, although both implantation types are energetically penalized, this penalty is considerably larger (0.65 eV) for the substitutional Ti. This explains the Ti_i concentration to be 50 times greater than Ti_{Si} in the experimental sample.

In addition, formation energies of double interstitial implantation were calculated, both considering the nearest (N) and remotest (R) possible Ti_i-Ti_i distance configurations,

$$E^f[Ti_iTi_iSi^R_{216}] = E[Ti_iTi_iSi^R_{216}] - E[Si_{216}] - E[Ti_2] = +2.99\ \text{eV},$$

$$E^f[Ti_iTi_iSi^N_{216}] = E[Ti_iTi_iSi^N_{216}] - E[Si_{216}] - E[Ti_2] = +2.63\ \text{eV}.$$

The formation energy of the remotest Ti_i-Ti_i configuration is almost twice the formation energy of a single interstitial Ti atom, as was expected. Although the balance for the nearest configuration is less unfavorable, due to the tendency of the Ti atoms to become aggregated in cluster form, the difference between both configurations is moderate, approximately 0.36 eV. Conversely, the formation energy of an interstitial implantation placed close to a substitutional Ti is

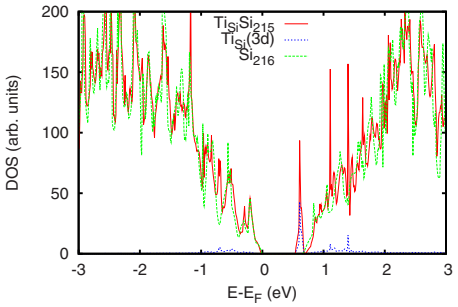

FIG. 2. (Color online) Total and Ti_{Si} $3d$ projected DOSs for the relaxed $Ti_{Si}Si_{215}$ compound compared with that from bulk Si_{216}.

$$E^f[Ti_iTi_{Si}Si^N_{215}] = E[Ti_iTi_{Si}Si^N_{215}] - \frac{215}{216}E[Si_{216}] - E[Ti_2] = +2.09\ \text{eV}.$$

Thus the formation energy of a dimer Ti_i-Ti_{Si} is not only much less unfavorable (0.54 eV) than a close Ti_i-Ti_i configuration but even smaller than the formation energy of a single substitutional Ti.

C. Electronic structure

1. Bulk Si

In a first step the electronic structures of the different bulk-Si unit cells were obtained. The indirect band gaps found correspond to 0.60 and 0.63 eV for the calculations carried out with the experimental and the relaxed structures, respectively. This means that the Si band gap was underestimated for nearly 50% of the experimental value (1.12 eV). These results are in agreement with other DFT-GGA calculations carried out in Si reports.[25,26] The bulk DOS will provide a reference to the different Ti-implanted situations proposed below.

2. Substitutional Ti

Band-structure calculations for the substitutional compound derived from the $2\times2\times2$-Si_8 supercell were carried out. In this cell the implantation, either substitutional or interstitial, of one Ti atom imposes a concentration $[Ti]=8\times10^{20}$ cm^{-3} which clearly exceeds the experimental situa-

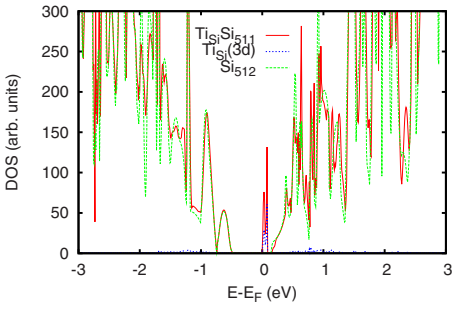

FIG. 3. (Color online) Total and Ti_{Si} $3d$ projected DOSs calculated for the nonrelaxed $Ti_{Si}Si_{511}$ compound compared with that from bulk Si_{512}.

TABLE III. Summary of results for bandwidth and possible electronic excitations obtained from the electronic structure of the compounds implanted with substitutional Ti. Results obtained after the correction of empty bands are in brackets. All values are given in eV.

Compound	e_g bandwidth	ΔE[VB−e_g]	ΔE[VB−CB]
$Ti_{Si}Si_{63}$	0.39	0.52(1.01)	0.81(1.30)
$Ti_{Si}Si_{215}$	0.15	0.54(1.03)	0.69(1.18)
$Ti_{Si}Si_{511}$	0.08	0.47(0.96)	0.62(1.11)

tion. Nevertheless, it was considered interesting to study these dilution levels in order to check whether an isolated intermediate band can be formed or if, on the contrary, the energy levels from the Ti 3*d* electrons overlap with any of the Si bands.

The $Ti_{Si}Si_{63}$ band structure shows that a doublet appears above the Fermi level (see Fig. 1), just slightly overlapping with the rest of the conduction band. The energy difference between the valence band maximum (VBM) and the conduction band minimum (CBM) is 0.81 eV, rather higher than 0.63 eV obtained for the host compound. Also a minor distortion in the CBM can be seen. The doublet has a bandwidth of 0.38 eV and its minimum is separated from the valence band by 0.52 eV. This low-energy e_g doublet, together with a high-energy triplet with t_{2g} symmetry, is originated from the crystal field splitting over the Ti 3*d* electrons that the tetrahedral environment imposes.[27,28] The four electrons coming from Ti_{Si} with valence 4+ arrange themselves as the sp^3 shell of the former Si atom. As a result, all the levels split from Ti 3*d* shell. The six remaining Ti 3*d* levels, corresponding to the t_{2g} triplets, are tightly hybridized with the CB.

The DOS of $Ti_{Si}Si_{215}$ ($[Ti]=2\times10^{20}$ cm^{-3}) shows, as in the case of the $Ti_{Si}Si_{63}$, both e_g doublets for each spin channel (see Fig. 2). Again these levels are empty while the remaining Ti 3*d* manifolds are again within the CB. There is a marked narrowing in the DOS at 0.69 eV above the VBM, which corresponds to a slight e_g-CB overlap. This energy difference is considerably smaller than that for the $Ti_{Si}Si_{63}$ but still greater than the one corresponding to the bulk Si. The bandwidth of the intermediate band is 0.15 eV and in this case is separated 0.54 eV from the VBM, similarly to the previous case.

A last interstitial Ti calculation for a $Ti_{Si}Si_{511}$ compound corresponding to 10^{20} cm^{-3} is carried out in order to check whether a split of the e_g manifolds from the CB is observed when approaching the Ti_{Si} concentration measured by Olea *et al.*[11] Although this value is still 2 orders of magnitude larger than the experimental amount of substitutional Ti, it is expected that the electronic structure at that dilution would be rather similar, except that the bandwidth of the potential IB formed would be slightly reduced.

The DOSs calculated for the $Ti_{Si}Si_{511}$ compound carried out are displayed in Fig. 3. The intermediate levels appear completely isolated from both VB and CB, conversely to the previous cases. The e_g doublets are placed 0.07 eV below the CBM and have a bandwidth of 0.08 eV. The resulting band gap is 0.62 eV, slightly higher than that of bulk Si.

From the results obtained above it is observed that substitutional Ti at dilution close to the experiment causes e_g manifolds to appear inside the host semiconductor band gap. However, they cannot produce by themselves any donor level because they are empty.

A brief summary of the main characteristics of the electronic structure found for the substitutional Ti at the different dilution levels is shown in Table III. Results considering a band-gap correction based on a rigid shift of 0.49 eV applied over empty bands have been included. The purpose of this correction is to recover the 1.12 eV VB-CB gap of bulk Si, which was found to be 0.63 eV in the previous GGA calculations. The rigid shift is carried out on the assumption that the possible changes induced by the Ti on the host semiconductor bands would not be significant.

3. Interstitial Ti

The most relevant quantitative features calculated from the electronic structure of interstitially Ti-implanted compounds are summarized in Table IV, where results with the same rigid shift of 0.49 eV than that applied in Table III have been included. In line with its atomic structure, the electronic structure of the interstitial compound is also more complex than that of the substitutional Ti. The effect of the octahedral crystal field originated by the six second nearest neighbors consists of splitting 3*d* levels into low-energy t_{2g} triplet and high-energy e_g doublet. This enters in competition with the tetrahedral crystal field from the four first nearest neighbors, as it was suggested by Ludwig and Woodbury.[29] As a result the overall influence of the second neighbors seems to be stronger. This fact is revealed by the band structure shown in Fig. 4. Both t_{2g} manifolds can be seen for each spin channel. These results for atomic relaxed compounds agree with previous theoretical works.[27,28] The filling of these levels produces a splitting between majority and minority t_{2g} triplets,

TABLE IV. Summary of results for bandwidths and possible electronic excitations obtained from the electronic structure of the compounds implanted with interstitial Ti. Arrows are referred to either majority (↑) or minority spin (↓) manifold. Results obtained after the correction of empty bands are in brackets. All values are given in eV.

Compound	$t_{2g}^{\uparrow}$ bandwidth	$t_{2g}^{\downarrow}$ bandwidth	ΔE[VB−$t_{2g}^{\downarrow}$]	ΔE[$t_{2g}^{\uparrow}$−CB]	ΔE[$t_{2g}^{\downarrow}$−CB]	ΔE[VB−CB]
Ti_iSi_{64}	0.49	0.65	0.78	−0.02 (0.47)	−0.09 (0.40)	0.71 (1.20)
Ti_iSi_{216}	0.17	0.28	0.62	0.19 (0.68)	0.00 (0.49)	0.63 (1.12)
Ti_iSi_{512}	0.06	0.11	0.49	0.30 (0.79)	0.11 (0.60)	0.61 (1.09)

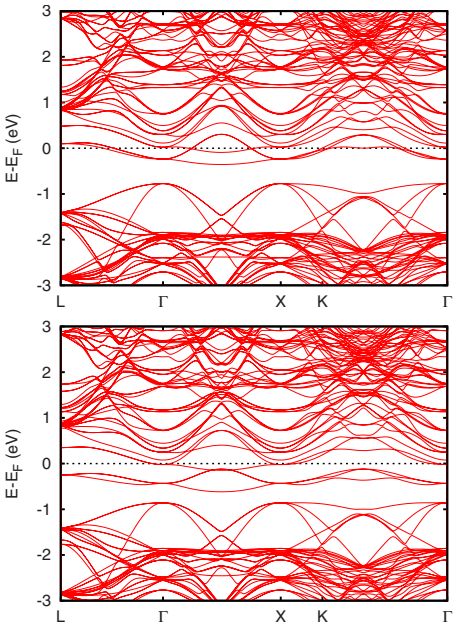

FIG. 4. (Color online) Minority (up) and majority (down) band structures obtained for the relaxed Ti_iSi_{64} compound.

with a full triplet emerging in minor contact with the host semiconductor CB and another one partially filled and overlapped with the CB more closely. The remaining Ti_i $3d$ levels appear mixed with higher conduction states. The energy difference between the VBM and the CBM is higher than the calculated semiconductor band gap, but the variation is less significant than that found for the $Ti_{Si}Si_{63}$ compound.

DOSs obtained for the interstitial Ti_iSi_{216} compound are shown in Fig. 5. A splitting similar to that found in the Ti_iSi_{64} compound can be appreciated. However, in this case the majority spin t_{2g} triplet is clearly isolated from the rest of the electronic levels and narrower than that calculated for the Ti_iSi_{64} case. The energy difference between the majority CBM and VBM almost coincides with the obtained for the host semiconductor band gap. Also, it can be seen that the minority manifold is narrower but not enough to be isolated from the CB. However, due to the well-known DFT underestimation of the band gap it is expected that describing the CB correctly at higher energies will separate it from the minority spin triplet.

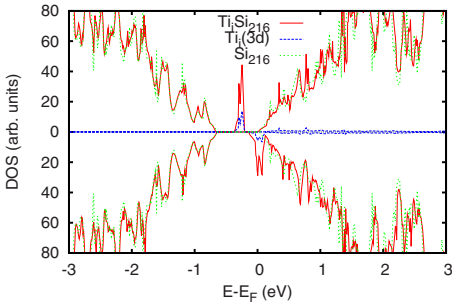

FIG. 5. (Color online) Total and Ti_i $3d$ projected DOSs for the relaxed Ti_iSi_{216} compound compared with that from bulk Si_{216}. From now on, majority and minority spin DOSs are represented in the upper and lower parts of the graph, respectively.

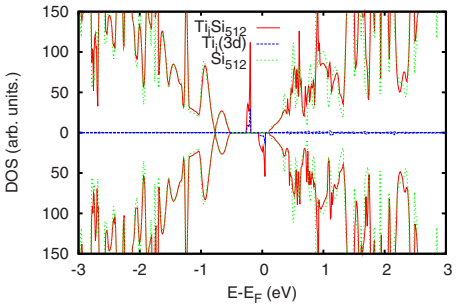

FIG. 6. (Color online) Total and Ti_i $3d$ projected DOSs calculated for the nonrelaxed Ti_iSi_{512} compound compared with that of bulk Si_{512}.

For the most diluted compound, Ti_iSi_{512} (see Fig. 6), both t_{2g} manifolds are completely isolated from both valence and conduction bands. The separation is caused by the narrowing of the intermediate bands. The majority and minority manifolds are 0.06 and 0.11 eV wide, respectively. The partially filled minority t_{2g} triplet, crossed by the Fermi energy, is separated 0.6 eV approximately from the CB after the band-gap correction. This value is similar to the result obtained by the simulation of the experimental results reported by Olea *et al.*[11] The host semiconductor band gap, 0.61 eV, corresponds almost exactly to the case of the (nonrelaxed) host Si_{512}.

4. Combination of interstitial and substitutional Ti implantations

In addition, other compounds with combined interstitial and substitutional Ti atoms were studied in order to verify where the energies of both Ti levels are located. A $Ti_{Si}Ti_iSi_{511}$ unit cell with both sites at the remotest relative positions was designed. The corresponding DOS (see Fig. 7) shows, as expected, that the electronic levels are rather similar to those of the noncombined unit cells. Only a small increase in the energies of the minority e_g doublet of the substitutional Ti atom was reported.

The dimer states produced when both impurities get closer modify, to some extent, the electronic structure shown in Fig. 8. A fully occupied majority spin triplet appears at only a few hundredths of eV above the valence band. Unlike the previous case, a half-filled doublet and an empty singlet are placed in the minority channel band gap. The doublet is

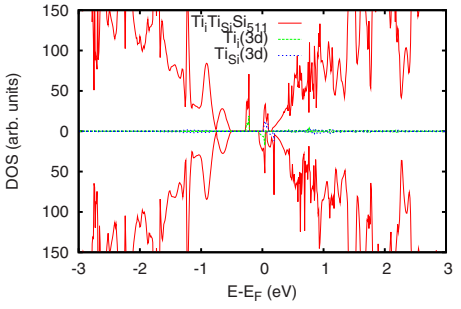

FIG. 7. (Color online) Total and partial (Ti_{Si} $3d$ and Ti_i $3d$) DOSs calculated for the $Ti_iTi_{Si}Si_{511}$ compound with both implanted Ti atoms located at the remotest sites.

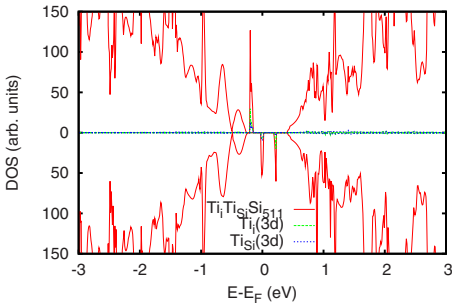

FIG. 8. (Color online) Total and partial (Ti_{Si} 3*d* and Ti_i 3*d*) DOSs calculated for the $Ti_iTi_{Si}Si_{511}$ compound with both implanted Ti atoms located at the nearest sites.

0.2 eV above the VBM and, in turn, the singlet is at 0.2 eV above the doublet. The band gap obtained in this calculation is slightly larger than that corresponding to the host semiconductor.

In principle, the existence of a donor level is compatible with this configuration, and even the half-filled doublet could correspond to an intermediate band. However, this close coexistence of both impurities is rather improbable. The reason lies in the fact that the relatively low concentration of Ti_i atoms should be combined with the much lower concentration of Ti_{Si} atoms.

D. Optical properties

We determined that the interstitial Ti seems to cause the experimental donor level and that it is a solid candidate to form an intermediate band inside the bulk-Si band gap. Therefore, its optical absorption coefficient has been studied to examine the enhancement of the absorption of the solar spectrum in comparison to bulk Si.

The Ti_iSi_{216} compound was selected to study the improvement in the optoelectronic properties given that it corresponds to the relaxed structure with the concentration closer to the experiment. Its absorption coefficient is shown in Fig. 9 together with that of bulk Si. In both cases a rigid shift has been applied over the eigenvalues of the CB in order to correct the GGA underestimation of the band gap. For bulk Si the main characteristics of the calculated absorption spectrum and those from the experimental results agree, except

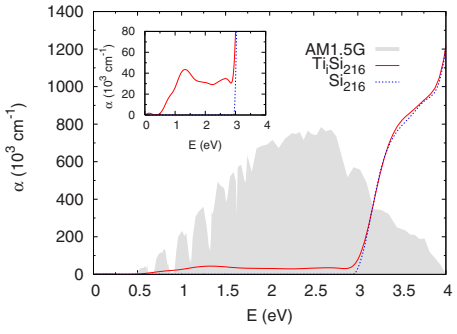

FIG. 9. (Color online) Optical absorption coefficient calculated for Ti_iSi_{216} and bulk-Si compounds. The solar spectrum AM1.5G (in arb. units) has been included as a solid shape in background.

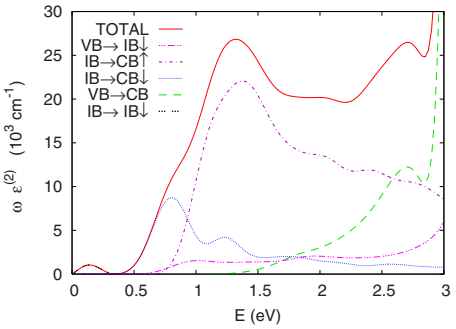

FIG. 10. (Color online) Imaginary part of the dielectric constant calculated for Ti_iSi_{216} compound. Both total and decomposed electronic transitions have been included. In the case of transitions from the VB to the CB (VB→CB) both spin components were added together as they had almost the same appearance.

for issues related to indirect transitions and exciton effects. The absorption of the Ti_iSi_{216} compound is enhanced in the energy range below 3 eV, in which the main part of the solar spectrum is contained.

The imaginary component of the dielectric constant and its different contributions have been examined (see Fig. 10) to verify the role of the IB in the absorption enhancement, given the close relationship between both properties. It can be seen that the main contribution below 3 eV is related to the IB levels. Apart from the intraband transitions, which are not relevant for photoconversion purposes, there is a peak at 0.8 eV resulting from electronic transitions from the minority IB to the CB. A bigger and broader peak appears centered at 1.4 eV. It is caused by the excitations from the majority IB manifold to the CB. The component originated by the transitions from VB to minority IB is modest throughout the studied range. Finally, a noticeable contribution resulting from low-energy transitions between VB and CB is observed. These are produced by the change from indirect to direct VB-CB gap as a result of small distortions in the CB states related to the appearance of the IB (see Fig. 2).

IV. SUMMARY AND CONCLUSIONS

It is revealed by the calculated energy balances that both interstitial and substitutional Ti implantation processes are unfavorable, in agreement with the difficulties in growing a crystalline structure without Ti clustering. However, interstitial Ti is less unstable by 0.65 eV, which explains the different concentration orders of magnitude found in the Ti-implanted samples of Olea *et al.*[11]

The full relaxation of atomic structures shows that substitutional Ti only introduces a small elongation of the interatomic distances from the tetrahedrally placed nearest neighbors. As a result two empty e_g-type doublets appear approximately at 0.5 eV above the valence band. In the most concentrated structures, GGA calculations show that these doublets are slightly overlapped with the CB. However, it is expected that a better description by correcting the band-gap underestimation of current calculations would increase both e_g and CBM energies to a similar degree, given that both bands are empty. Therefore, we consider that the substitu-

tional Ti would provide an empty band approximately at a few tenths of eV below the conduction band edge. However, the level found through the experiments, being donor, cannot be attributed to these empty states.

Although the interstitially implanted Ti atom relaxes into a site tetrahedrally coordinated by four Si atoms, its second nearest neighbors are sited at octahedral positions just slightly further away, establishing a competition between both crystalline field trends. The low-energy triplets found in the DOS suggest that the main interaction corresponds to the octahedral environment. At an experimental Ti_i concentration, both majority and minority t_{2g} manifolds are found by the DFT-GGA calculations completely isolated between themselves and the Si CB, the partially filled minority triplet being at 0.11 eV below the CBM. Extrapolating the position of the CB by applying a rigid shift, the minority t_{2g} manifold would be located at approximately 0.5 eV below the CB. In summary, the presence of interstitial atoms is enough to generate the donor state found through the experiments.

The influence of other nearby (interstitial or substitutional) Ti atoms could have some effect on the position of the donor level. In the case of coexistence of close Ti-implanted atoms, the energy balances suggest that the Ti_{Si}-Ti_i dimer is much less unfavorable than Ti_i-Ti_i or Ti_{Si}-Ti_{Si}. In any case, this kind of dimers is rather unlikely in samples with a Ti dilution of around 5×10^{19} cm^{-3}.

Besides that a method beyond DFT could set accurately the position of the electronic levels, we argue that the origin of the donor state found in the experimental Ti-implanted Si samples settles from the interstitial Ti. Its isolated partially filled manifold complies with the requirements needed to behave as an appropriate intermediate-band photovoltaic material. This fact, together with the lower energy formation of interstitial Ti compared with other kind of Ti implantation products, allows the assumption that the manufacture of an intermediate-band solar cell is feasible. The effect of the intermediate band present in the Ti_iSi_{216} compound over the absorption coefficient of bulk Si implies a significant enhancement of the optical absorption in an important part of the incoming solar spectrum, caused essentially by electronic excitations involving the IB.

ACKNOWLEDGMENTS

We would like to acknowledge funding from the GENESIS-FV (Grant No. CSD2006-0004) and the CALIBAND (Grant No. MAT2006-10618) projects of the Spanish Ministry of Education and Science and from the NUMANCIA-MA (Grant No. S-05050/ENE/0310) project of the Community of Madrid. We acknowledge the computer resources and assistance provided by the Centro de Supercomputación y Visualización de Madrid (CeSViMa).

[1] A. Luque and A. Martí, Phys. Rev. Lett. **78**, 5014 (1997).
[2] P. Wahnón and C. Tablero, Phys. Rev. B **65**, 165115 (2002).
[3] P. Palacios, J. J. Fernández, K. Sánchez, J. C. Conesa, and P. Wahnón, Phys. Rev. B **73**, 085206 (2006).
[4] P. Palacios, K. Sánchez, J. C. Conesa, and P. Wahnón, Phys. Status Solidi A **203**, 1395 (2006).
[5] P. Palacios, I. Aguilera, K. Sánchez, J. C. Conesa, and P. Wahnón, Phys. Rev. Lett. **101**, 046403 (2008).
[6] K. M. Yu, W. Walukiewicz, W. Shan, J. Wu, J. W. Beeman, M. A. Scarpulla, O. D. Dubon, and P. Becla, J. Appl. Phys. **95**, 6232 (2004).
[7] K. M. Yu, W. Walukiewicz, J. W. Ager III, D. Bour, R. Farshchi, O. D. Dubon, S. X. Li, I. D. Sharp, and E. E. Haller, Appl. Phys. Lett. **88**, 092110 (2006).
[8] P. Palacios, P. Wahnón, S. Pizzinato, and J. C. Conesa, J. Chem. Phys. **124**, 014711 (2006).
[9] R. Lucena, I. Aguilera, P. Palacios, P. Wahnón, and J. C. Conesa, Chem. Mater. **20**, 5125 (2008).
[10] A. S. Brown and M. A. Green, J. Appl. Phys. **96**, 2603 (2004).
[11] J. Olea, M. Toledano-Luque, D. Pastor, G. González-Díaz, and I. Mártil, J. Appl. Phys. **104**, 016105 (2008).
[12] A. Luque, A. Martí, E. Antolín, and C. Tablero, Physica B **382**, 320 (2006).
[13] J. Olea, G. G. Díaz, D. Pastor, and I. Mártil, J. Phys. D: Appl. Phys. **42**, 085110 (2009).
[14] P. Hohenberg and W. Kohn, Phys. Rev. **136**, B864 (1964).
[15] W. Kohn and L. J. Sham, Phys. Rev. **140**, A1133 (1965).
[16] J. P. Perdew, J. A. Chevary, S. H. Vosko, K. A. Jackson, M. R. Pederson, D. J. Singh, and C. Fiolhais, Phys. Rev. B **46**, 6671 (1992).
[17] G. Kresse and J. Hafner, Phys. Rev. B **47**, 558 (1993).
[18] G. Kresse and J. Furthmüller, Phys. Rev. B **54**, 11169 (1996).
[19] P. E. Blöchl, Phys. Rev. B **50**, 17953 (1994).
[20] G. Kresse and D. Joubert, Phys. Rev. B **59**, 1758 (1999).
[21] M. Methfessel and A. T. Paxton, Phys. Rev. B **40**, 3616 (1989).
[22] P. E. Blöchl, O. Jepsen, and O. K. Andersen, Phys. Rev. B **49**, 16223 (1994).
[23] M. Gajdoš, K. Hummer, G. Kresse, J. Furthmüller, and F. Bechstedt, Phys. Rev. B **73**, 045112 (2006).
[24] J. Furthmüller, http://www.freeware.vasp.de/VASP/optics.
[25] S. A. Harrison, T. F. Edgar, and G. S. Hwang, Phys. Rev. B **74**, 195202 (2006).
[26] W. a. L. Scopel, A. J. R. da Silva, and A. Fazzio, Phys. Rev. B **75**, 193203 (2007).
[27] H. Katayama-Yoshida and A. Zunger, Phys. Rev. B **31**, 8317 (1985).
[28] F. Beeler, O. K. Andersen, and M. Scheffler, Phys. Rev. B **41**, 1603 (1990).
[29] G. W. Ludwig and H. H. Woodbury, Phys. Rev. Lett. **5**, 98 (1960).